International Journal of Minerals, Metallurgy and Materials
Volume 18, Number 4, August 2011, Page 419
DOI: 10.1007/s12613-011-0456-3

Microstructure and embrittlement of the fine-grained heat-affected zone of ASTM4130 steel

Li-ying Li, Yong Wang, Tao Han, and Chao-wen Li

College of Mechanical and Electronic Engineering, China University of Petroleum, Dongying 257061, China
(Received: 31 July 2010; revised: 8 October 2010; accepted: 15 October 2010)

Abstract: The mechanical properties and microstructure features of the fine-grained heat-affected zone (FGHAZ) of ASTM4130 steel was investigated by optical microscope (OM), scanning electron microscope (SEM), transmission electron microscope (TEM), and welding thermal simulation test. It is found that serious embrittlement occurs in the FGHAZ with an 81.37% decrease of toughness, compared with that of the base metal. Microstructure analysis reveals that the FGHAZ is mainly composed of acicular, equiaxed ferrite, granular ferrite, martensite, and martensite-austenite (M-A) constituent. The FGHAZ embrittlement is mainly induced by granular ferrite because of carbides located at its boundaries and sub-boundaries. Meanwhile, the existence of martensite and M-A constituent, which distribute in a discontinuous network, is also detrimental to the mechanical properties.

Keywords: ASTM4130 steel; welding; heat-affected zone; microstructure; embrittlement

[*This work was financially supported by the National High-Tech Research and Development Program of China (No.2006AA09A103-6).*]

1. Introduction

ASTM 4130 steel exhibits high strength and excellent low temperature toughness, and has been extensively used for oil and gas production, such as high-pressure pipelines of deep-water semi-submersible drilling platforms [1]. Generally, the mechanical properties of the heat-affected zone (HAZ) are different from those of the base metal (BM) due to the effect of thermal cycles. Extensive studies on the high strength low alloy (HSLA) steels have shown that the lowest toughness of the coarse-grained HAZ (CGHAZ) [2-5] and the intercritical HAZ (ICHAZ) [6-7] is found in single pass welding. However, only limited literatures have demonstrated that the toughness of fine-grained HAZ (FGHAZ) is much lower than that of BM. Additionally, since HAZ is generally narrow and discontinuous, a weld thermal simulator is often employed to produce a large volume of uniform microstructure, which is suitable for microstructure and mechanical properties assessments. Therefore, the aim of the present work is to analyze the correlation between the microstructure and mechanical properties of the FGHAZ of ASTM4130 steel by means of a welding simulation technique.

2. Materials and methods

The ASTM4130 steel pipe used in the experiment is ϕ141.3 mm×30 mm, and the measured chemical composition is listed in Table 1.

Table 1 Chemical composition of tested ASTM4130 steel

wt%

C	Si	Mn	Cr	Mo	Ni	S	P	Fe
0.32	0.355	0.62	1.15	0.25	0.17	0.004	0.010	balance

Square bar specimens (10.5 mm×10.5 mm×80 mm) for thermal cycle simulation were cut along the axial direction parallel to the pipe. The welding simulation parameters are as follows: preheat temperature 200°C, welding heat input 20 kJ/cm, heating velocity 130°C/s, peak temperature 950°C, and holding time 2 s.

After simulation test, the specimens were machined into

Corresponding author: Li-ying Li E-mail: llying3456@163.com

standard V-notch Charpy specimens of 10 mm×10 mm×55 mm, and the toughness was evaluated at −30°C. The microstructures were observed by optical microscopy (OM) and transmission electron microscopy (TEM). Hardness was measured under the load of 10 kg and 25 g, respectively.

3. Results and discussion

3.1. Properties of FGHAZ

FGHAZ properties of ASTM4130 steel are shown in Fig. 1. It can be seen apparently that a severe embrittlement phenomenon occurs in the FGHAZ. The Charpy energy of FGHAZ is only 35.02 J, with a decrease of 81.37% compared with BM. However, the hardness increases from Hv_{10} 252.4 to Hv_{10} 315.1, with an increase of 24.84%. Fig. 2 illustrates the load-displacement curve of the instrumented impact tests of the FGHAZ. The area of OF_mS_m indicates the crack initiation energy (E_i), the area of $F_mS_mS_t$ indicates the crack propagation energy (E_p), and the sum of both is the total impact energy (E_t). In this case, E_i, E_p and E_i are 34.02, 0.03, and 34.05 J, respectively. Namely, it is noted that the FGHAZ toughness is deteriorated, which is indicated by the low ratio of E_p/E_i and E_p/E_t [8].

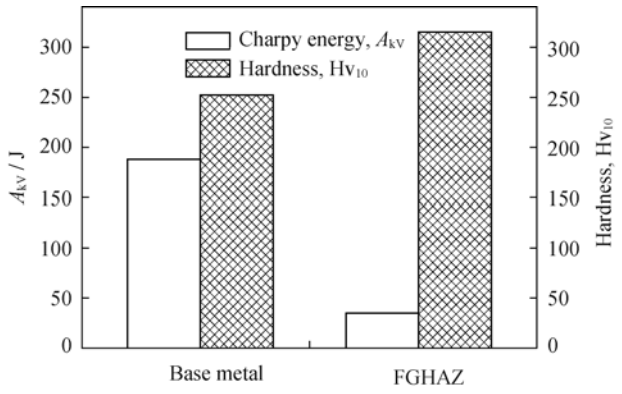

Fig. 1. Properties of FGHAZ.

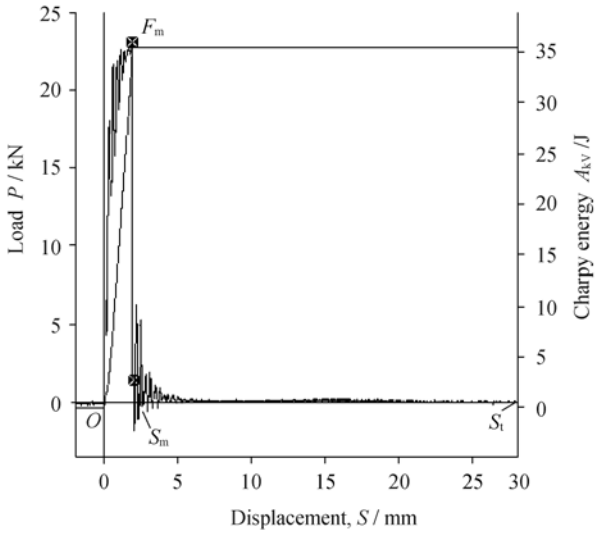

Fig. 2. Load-displacement curve of FGHAZ.

3.2. Microstructures of FGHAZ

Fig. 3 depicts optical micrographs of the FGHAZ etched by a 4vol% nitric solution and two-step metallographic etching technology [9], respectively. As can be seen, it mainly contains acicular and equiaxed ferrite, as well as granular microstructure, but does not seem to contain much martensite (Fig. 3(a)). However, in Fig. 3(b), the white islands of martensite and martensite-austenite (M-A) constituent are found, which cannot be distinguished [5, 10], while the gray is ferrite. Microhardness measurement illustrates that ferrite and martensite are $Hv_{0.025}$ 217.2 and $Hv_{0.025}$ 479.1, respectively.

Fig. 4 is a group of TEM micrographs of the FGHAZ. The substructure of the equiaxed ferrite is the low density dislocation (Fig. 4(a)). The granular microstructure is also ferrite confirmed by selected area electron diffraction spots (Fig. 4(b)). Carbides (M_3C) can be found to locate at the boundaries and sub-boundaries. TEM analysis also reveals that the FGHAZ includes dislocation and twinning martensite mostly existing at the prior austenite boundaries, as shown

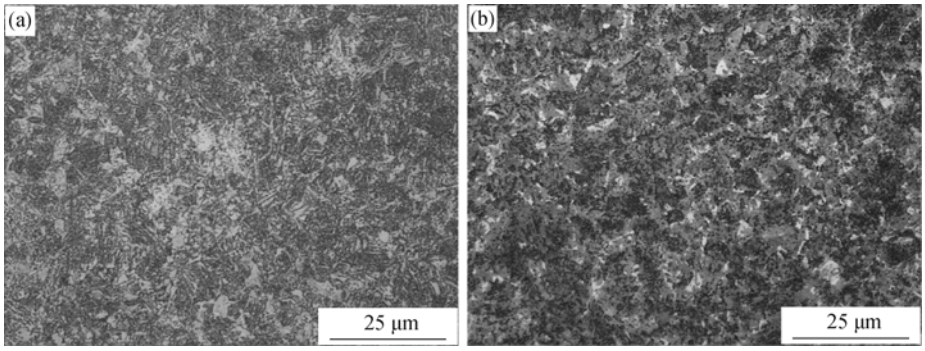

Fig. 3. Optical micrographs of FGHAZ etched by a 4vol% nitric solution (a) and two-step metallographic etching technique (b).

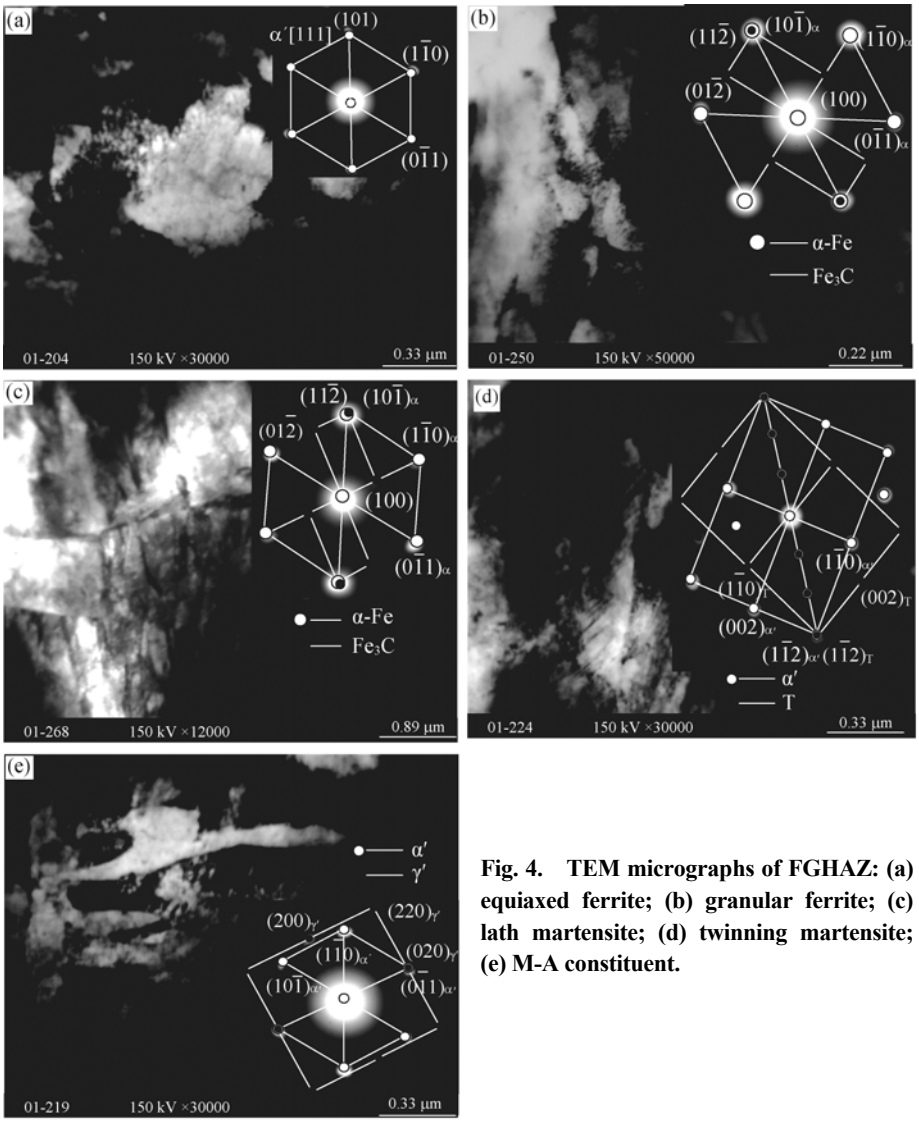

Fig. 4. TEM micrographs of FGHAZ: (a) equiaxed ferrite; (b) granular ferrite; (c) lath martensite; (d) twinning martensite; (e) M-A constituent.

in Figs. 4(c)-(d). Carbides are also found to locate within lath and along lath boundaries. Besides, M-A constituent is confirmed to appear in the FGHAZ (Fig. 4(e)). It is evident that microstructures of the FGHAZ, in the order of dislocation density from low to high, are acicular, equiaxed ferrite, granular ferrite, martensite, and M-A constituent.

The FGHAZ consists of not only martensite but also a considerable amount of ferrite. This is inconsistent with the continuous cooling temperature (CCT) curve. The reason might lie in the following factors. One is the fine grain of prior austenite. The finer the prior austenite grain is, the more unstable the super cooled austenite becomes. Thus, the presence of fine grain austenite makes it possible for ferrite to form at a higher temperature. This is in good agreement with conclusions drawn from Ref. [11]. The other is the uniform chemical composition of the prior austenite.

Fig. 5(a) is a schematic illustration of nucleation and growth of austenite. The austenite primarily nucleates at the boundaries of ferrite, and then grows along the boundaries in the shape of first strip and secondly near-connected network, expanding into the interior of the ferrite grain [12]. When cooled, it first transforms into acicular and equiaxed ferrite, then granular ferrite, and finally martensite and M-A constituent, as shown in Fig. 5(b). The first nucleation sites are within austenite grains, rather than along the austenite boundaries, which contradicts with the conventional viewpoint. This is closely related to the presence of undissolved carbides that can act as the core of non-homogeneous nucleation. The transformation sequence can be testified by microstructural features (Fig. 4) since the dislocation density of the microstructure formed at a higher temperature is lower than that formed at a lower temperature.

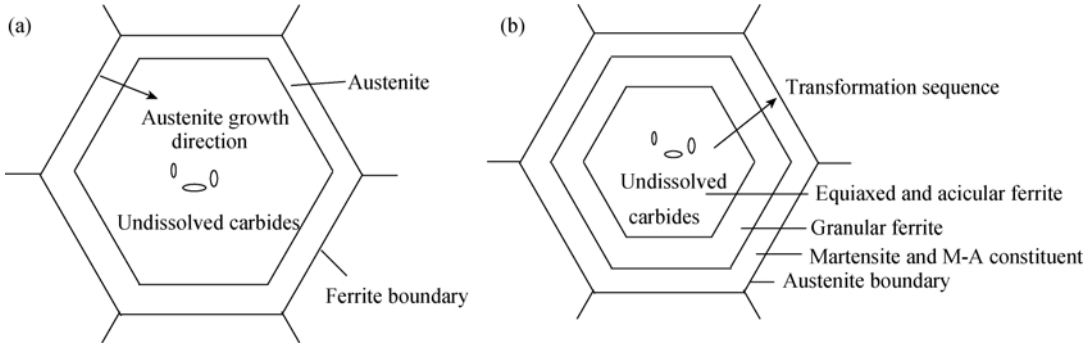

Fig. 5. Schematic illustration: (a) nucleation and growth of austenite; (b) microstructure transformation as cooled.

3.3. Embrittlement analysis

Based on the above analysis, it can be found that the FGHAZ toughness of ASTM4130 steel decreases sharply, which hardly occurs in most HSLA steels. In this case, the reasons might be as follows.

(1) The existence of equiaxed ferrite. When it is suffering from an external force, the equiaxed ferrite preferentially deforms, then the crack initiates along its boundary due to the inconsistency with the deformation of adjacent microstructure, thereby inducing deterioration in toughness [13].

(2) Distribution feature of martensite and M-A constituent. Refs. [14-15] indicate that blocky M-A constituent distributed in a near-connected grain boundary network has maximal adverse effect on impact toughness.

(3) The existence of granular ferrite. Carbides distributed at the boundaries and sub-boundaries are similar to the brittle second phase surrounding the soft. The hardening phase separates the plastic phase in the space, so that deformation is unable to play fully, thus making the crack initiate and propagate along the grain boundary after a small amount of deformation, thereby resulting in the toughness decreasing sharply.

As can be seen in Fig. 6, the crack initiates from a plane that is inside the grain, and propagates outwards, then fractures along the prior austenite boundary in a quasi-cleavage mode. It is obvious that dimple walls are smooth. This means that low energy is consumed. Thus, fractographic examination, coupled with microstructural features, has revealed that the brittle fracture initiates at granular ferrite, rather than M-A constituent. However, the presence of M-A constituent located along the grain boundaries provides a low-energy channel for crack propagation.

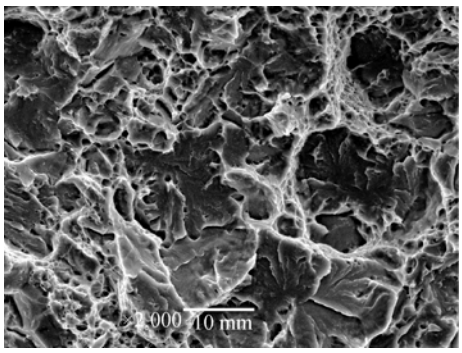

Fig. 6. SEM fractograph of FGHAZ.

4. Conclusions

(1) Contrary to the traditional view, serious embrittlement occurs in the FGHAZ of ASTM4130 steel, with its toughness decreasing 81.37%, compared with that of the base metal.

(2) The FGHAZ of ASTM4130 is mainly composed of acicular, equiaxed ferrite, granular ferrite, martensite, and M-A constituent. The martensite and M-A constituent are located along the prior austenite boundaries.

(3) The main factor controlling the toughness of FGHAZ is granular ferrite with carbides located at the boundaries and sub-boundaries of the ferrite. In addition, the presence of M-A constituent also results in the toughness deterioration.

References

[1] J.R. Still, Welding of AISI 4130 and 4140 steel for drilling systems, *Weld. J.*, 76(1997), No.6, p.37.

[2] Y.H. Chen, Y. Wang, and B. Han, Metallurgical microstructure and fine structure in local brittle zone of in-service welding of X70 pipeline steel, *Trans. Mater. Heat Treat.*, 28(2007), No.1, p.79.

[3] E. Bonnevie, G. Ferrière, A. Ikhlef, D. Kaplan, and J.M. Oraina, Morphological aspects of martensite-austenite constituents in intercritical and coarse grain heat affected zones of structural steels, *Mater. Sci. Eng. A*, 385(2004), No.1-2, p.352.

[4] G.S. Duan, W.Q. Chen, and B. Sun, Impact toughness in the welding heat affected zone of HSLA steel with boron, *J. Univ. Sci. Technol. Beijing* (in Chinese), 31(2009), No.8, p.995.

[5] B.C. Kim, S. Lee, N.J. Kim, and D.Y. Lee, Microstructure and local brittle zone phenomena in high-strength low-alloy steel welds, *Metall. Trans. A*, 22(1991), No.1, p.139.

[6] Y.J. Li, Z.D. Zou, H.Q. Wu, and J. Wang, Microstructure and performance in the inter-critical region of heat-affected zone of HQ130 steel, *Trans. China Weld. Inst.*, 22(2001), No.2, p.54.

[7] M. Eroglu and M. Aksoy, Effect of initial grain size on microstructure and toughness of intercritical heat-affected zone of a low carbon steel, *Mater. Sci. Eng. A*, 286(2000), No.2, p.289.

[8] F. Zia-Ebrahimi and G. Krauss, The evaluation of tempered martensite embrittlement in 4130 steel by instrumented charpy V-notch testing, *Metall. Trans. A*, 14(1983), No.5, p.1109.

[9] R.M. Alé, J.M.A. Rebello, and J. Charlier, A metallographic technique for detecting martensite-austenite constituents in the weld heat-affected zone of a micro-alloyed steel, *Mater. Charact.*, 37(1996), No.2-3, p.89.

[10] S. Lee, B.C. Kim, and D. Kwon, Correlation of microstructure and fracture properties in weld heat-affected zones of thermomechanically controlled processed steels, *Metall. Trans. A*, 23(1992), No.10, p.2803.

[11] G. Spanos, R.W. Fonda, R.A. Vandermeer, and A. Matuszeski, Microstructural changes in HSLA-100 steel thermally cycled to simulate the heat-affected zone during welding, *Metall. Mater. Trans. A*, 26(1995), No.12, p.3277.

[12] Y.P. Kang, *Metallic Solid Phase Transition and Application*, Chemical Industry Press, Beijing, 2008, p.18.

[13] H.L. Gao, Study of strength and toughness of over-heated HAZ in medium carbon Q and T steel, *Trans. China Weld. Inst.,* 15(1994), No.2, p.107.

[14] C.L. Davis and J.E. King, Cleavage initiation in the intercritically reheated coarse-grained heat-affected zone: Part I. Fractographic evidence, *Metall. Mater. Trans. A*, 25(1994), No.3, p.563.

[15] S.F. Yu and B.N. Qian, Local brittleness of X70 pipeline steel, *Chin. J. Mater. Res.*, 18(2004), No.4, p.405.